STUDIA UBB CHEMIA, LXIX, 4, 2024 (p. 21-35)
(RECOMMENDED CITATION)
DOI:10.24193/subbchem.2024.4.02

ELECTROCHEMICAL CHARACTERIZATION AND DNA INTERACTION STUDIES OF A NOVEL COPPER SCHIFF BASE COMPLEX: INSIGHTS FROM CYCLIC VOLTAMMETRY AND MOLECULAR DOCKING

Chahinaz ZOUBEIDI[a], Ali OURARI[b], Elhafnaoui LANEZ[c], and Touhami LANEZ[c,*]

ABSTRACT. In this study, we investigate the electrochemical properties of a novel copper complex (CuL_2) derived from the Schiff base ligand N-3-bromopropylsalicylaldimine (LH). We also examine its interaction with chicken blood double-stranded DNA (cb-ds DNA) in phosphate buffer solution (PB) at physiological pH 7.2 using cyclic voltammetry (CV) techniques. The interaction mechanism of nitrite with CuL_2, involving the CuII/CuI redox system, is explored. The CuL_2 complex was electropolymerized on glassy carbon (GC) and fluorine tin oxide (FTO). The morphology of PolyCuL_2 formed on FTO was analyzed using scanning electron microscopy (SEM) and its elemental composition determined by EDX analysis. The modified electrode polyCuL_2/GC exhibited efficient catalytic activity for the electroreduction of oxygen (O_2) in homogeneous electrocatalytic media. The binding constant (Kb) of the DNA-CuL_2 adduct, determined from CV measurements, was found to be 1.33×10^5, closely matching the value obtained from molecular docking studies (1.75×10^5). Docking studies indicate that the CuL_2 complex binds to DNA in the minor groove binding mode. The anodic peak potential shift in the negative direction suggests an electrostatic interaction between CuL_2 and DNA.

Keywords: *Copper(II) complex; Electro-polymerization; catalytic reduction; DNA binding affinity; AutoDock.*

[a] *Department of Renewable Energies, Faculty of Hydrocarbons, Renewable Energies and Earth and Universe Sciences, University of Ouargla, BP.511, 30000, Ouargla, Algeria*
[b] *Laboratory of Electrochemistry, Molecular Engineering and Redox Catalysis (LEIMCR), Faculty of Technology, Ferhat ABBAS University of Sétif-1, Sétif 19000, Algeria*
[c] *VTRS Laboratory, Department of Chemistry, Faculty of Sciences, University of El Oued, B.P.789, 39000, El Oued, Algeria*
* *Corresponding author: touhami-lanez@univ-eloued.dz*

©2024 STUDIA UBB CHEMIA. Published by Babeş-Bolyai University.

This work is licensed under a Creative Commons Attribution-NonCommercial-NoDerivatives 4.0 International License.

INTRODUCTION

Numerous Schiff base ligands have been investigated as starting materials for coordinating transition metals. The increased interest in their metal complexes is due to their usefulness in various fields. A new class of ligands containing two coordination sets (N and O atoms) with a carbon-bromide function (C-Br) has garnered attention due to their prominent chemical reactivity [1–3].

Moreover, there has been growing interest in the synthesis, characterization, and crystal structures of Cu(II) Schiff base complexes [2–6]. These complexes exhibit interesting properties and structural diversity, making them useful for many applications[7,8], including the preparation of supramolecular assemblies[9,10] and the development of highly sensitive carbon paste electrodes modified with copper complexes for electrocatalytic reduction of nitrite (NO_2^-) [11] and bromate (BrO_3^-) in aqueous media [12].

Transition metal coordination compounds have been extensively used as DNA structural probes [13], DNA cleaving agents [14], DNA molecular light switches [15], and for various other applications [16,17]. They form very stable complexes with peculiar properties and reactivity, particularly in binding small molecules [18,19]. These chelating ligands with O and N donor atoms and their complexes also show broad biological activity [20,21]. Furthermore, some dibromide-bridged binuclear Cu(II) complexes, based on Schiff base ligands, have been investigated for their potential as anticancer agents [22,23].

Continuing from our previous work, where the Cu(II) complex and its ligand were characterized by microanalysis, UV–Vis, FT-IR, ^{1}H NMR, and ^{13}C NMR spectroscopy, with structures confirmed by single crystal X-ray crystallography[24], we now report on the investigation of the electrocatalytic properties of a new copper Schiff base complex (CuL_2). This complex appears in polymer matrices as pendant functional groups covalently grafted by bromide atoms. We also examine the interaction of CuL_2 with chicken blood double-stranded DNA using cyclic voltammetry (CV) techniques and molecular docking simulation.

RESULTS AND DISCUSSION

The ligand LH was synthesized by reacting 3-bromopropylamine hydrobromide with 2-hydroxybenzaldehyde in a 1:1 molar ratio, using a base to enhance the nucleophilicity of the amino group ($-NH_2$)[24]. The CuL_2 complex was then prepared by refluxing the ligand with Cu(II) acetate tetrahydrate in

absolute ethanol, resulting in a dark green precipitate from the exchange reaction between LH and the copper salt. The reaction pathways for the formation of LH and the CuL_2 complex are shown in Schemes 1 and 2.

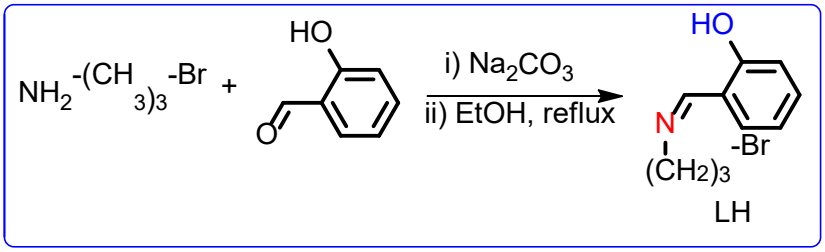

Scheme 1. Synthetic route of Schiff base ligand LH.

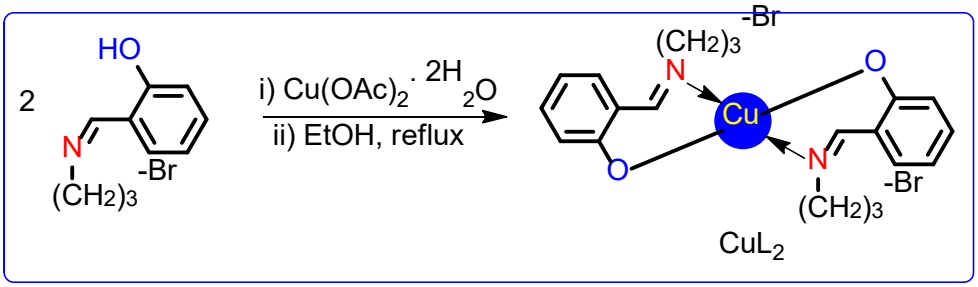

Scheme 2. Synthetic route of Schiff base-copper complex CuL_2.

Electrochemical study of CuL_2 complex

The CuL_2 complex was investigated using cyclic voltammetry in an acetonitrile solution with a scan rate of 100 $mV.s^{-1}$, within the potential range of -1.80 to 1.80 V against a Saturated Calomel Electrode (SCE).

Upon sweeping the voltage to oxidizing potentials, CuL_2 (Figure 1) shows two anodic waves at +1.08 (I) and +1.24 V (II). The first peak (I) corresponds to the quasi-reversible oxidation of the Cu(II) to Cu(III) [6, 25]. LH_2, being the most electron donating as the dianionic form/ $(L^-)_2$, stabilizes the copper ion in the higher oxidation state Cu(III) and disfavors reduction of the copper(II) cation. The active species of Cu (III) is likely to oxidize the ligand LH_2 via an intermediate electron transfer process, by electrochemical reaction with ligand Schiff base. The second peak (II) is observed at nearly the same potential value as the corresponding ligand and can be attributed

to irreversible oxidation of phenolic groups of the ligand [1,6,26]. LH_2, being the most electron donating as the dianionic $(L^-)_2$, stabilizes the copper ion in the higher oxidation state and disfavors reduction of the copper(II) cation. Also, the oxidation potential of the cooper complex seems to be more positive than the value observed for the ligand, which may be related to the relative stability of the coordination bonding between the oxygen and the azote atom with copper (II) ion. Two overlapping reduction peaks at -0.78 (III) and -1.07(IV) V/SCE, which are assigned to the Cu(II)/Cu(I) redox couple and the reduction the imine groups of the Schiff base, respectively [25]. The latter reduction wave is significantly shifted to less cathodic potentials compared to the ligand alone, indicating a decrease in the electron density of the imine group after the coordination process with the copper complex [28].

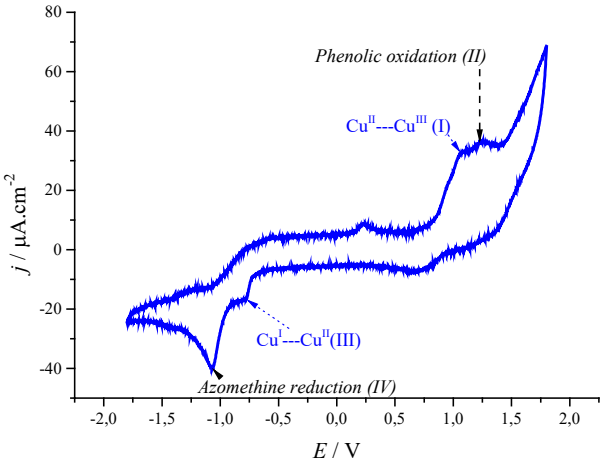

Figure 1. Cyclic voltammogram of 1 mM of CuL_2 at GC electrode in acetonitrile solution 0.1 M TBAP. Scan rate 100 $mV.s^{-1}$.

Figure 2 displays a pair of oxidation-reduction peaks corresponding to the Cu(III)/Cu(II) redox couple at1.08 V and 0.64 V. The ΔEp data being larger than the theoretical value for an electrochemically reversible one-electron process. Thus, for this complex the large ΔEp value expressing an electrochemical oxidation of Cu(II) would be due to a quasi-reversible behavior of the couple Cu(III)L + e− = Cu(II)L yielding an average formal potential of $E_{1/2}$ = 0.86 V. The difference between the anodic and cathodic potentials is ΔEp1 = 0.44 V and the current ratio (Ipc_3/Ipa_3) exceeds unity at 4.83 confirm the irreversibility electrochemistry of this redox couple.

The Cu(III)/Cu(II) redox couple appears to be scan-rate-dependent, particularly for the anodic wave. At lower scan rates (10-100 mV.s^{-1}), this anodic wave splits into two. As the scan rate increases, the first wave shifts to more anodic potentials, while the second wave shifts to more cathodic potentials, resulting in an increase in current intensities. These two redox couples are likely irreversible, consistent with previous reports in the literature [29,30].

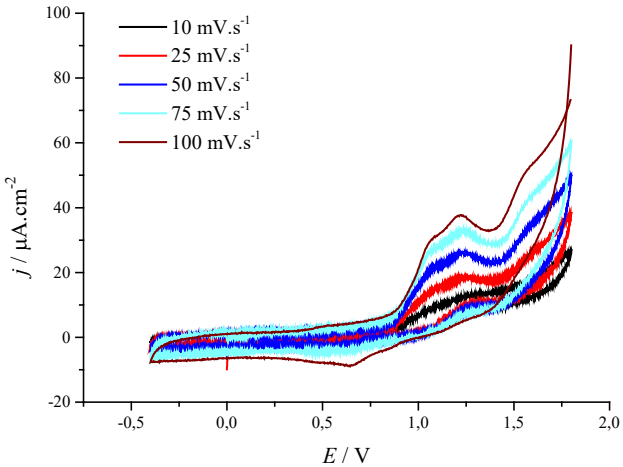

Figure 2. Cyclic voltammogram of 1 mM CuL_2 in 0.1 M TBAP/CH_3CN showing scan rate dependence of Cu(II) / Cu(III) redox couple.

The electroreduction polymerization process of the copper complex CuL_2 on optically transparent electrodes was observed by a continuous increase in peak currents during the initial cathodic sweep scans (Figure 3A). In subsequent scans, the current decreases, and after several cycles, the initial reduction peaks disappear, replaced by two new peaks around -0.6 V/SCE, indicating the formation of a deposited film on the electrode surface. These redox processes correspond to the Cu(II)/Cu(I) redox couple and increase with the number of cycles [31,32]. As the number of cycles increases, not only does the peak current intensity rise, but the potential also shifts to more negative values [33,34]. It has been proposed that the oxidative polymerization of Salen-type metal units is primarily a ligand-based process, where radical–radical coupling between the phenol rings is responsible for polymer formation. This new material can be considered a modified electrode [PolyCuL_2/GC]. Comparing the electrochemical processes, such as anodic oxidation or cathodic reduction, the monomer involved in these reactions leads to the formation of intermediate radical-cations and radical-anions, respectively (see Eq. 1 and Eq. 2).

$$CuL_2 - e^- \rightarrow [CuL_2]^+ \quad (1)$$

$$CuL_2 + e^- \rightarrow [CuL_2]^- \quad (2)$$

Similarly, the electrochemical process described in Eq. 2 initially produces radical-anions. These radical species participate in radical-radical coupling, resulting in the formation of polymer films and thereby producing modified electrodes [33,34]. The PolyCuL$_2$ film is deposited and grows on an optically transparent FTO-coated glass electrode, as evidenced by the continuous increase in the peak currents of the copper complex (Figure 3B).

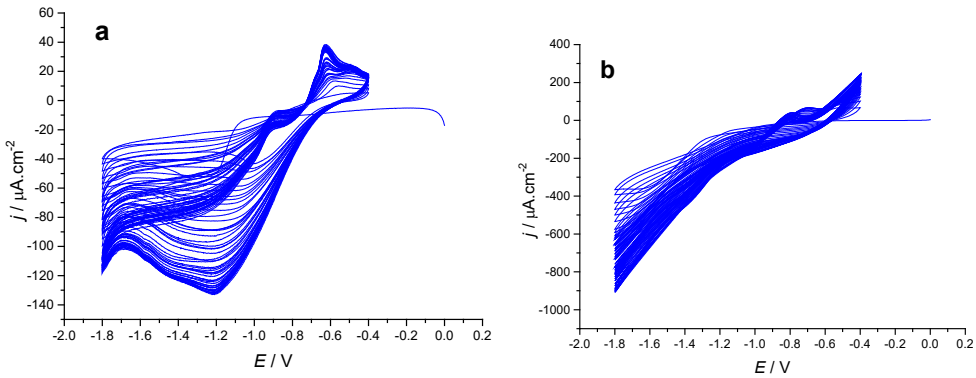

Figure 3. (a) Cyclic voltammogram showing electropolymerization of 0.1 M of CuL$_2$, 0.1 M TBAP/CH$_3$CN by: cycling between -0.4 and -1.8 V/SCE in acetonitrile solution using GC-electrode at 75 Mv. s^{-1} in (100 cycles). **(b)** and FTIO electrode at 100 mV s-1 (100 cycles).

Energy dispersive X-ray (EDS) analysis of the PolyCuL$_2$/FTO was conducted to investigate the adsorption of Cu on the surface of the modified electrode within the polymer catalyst structure (Figure 4). The EDS images display peaks corresponding to copper, oxygen, and nitrogen, confirming the presence of these elements. Furthermore, the analysis indicated that the coating of copper on the surface of the modified electrode PolyCuL$_2$ was successful.

The scanning electron microscopy (SEM) images presented in Fig. 5 were used to explore the morphology of the film electropolymerized onto an FTO substrate. The surface of the PolyCuL$_2$ film, obtained by cycling 100 times between -0.4 and -1.8 V, displays high porosity, which becomes apparent at high magnifications.

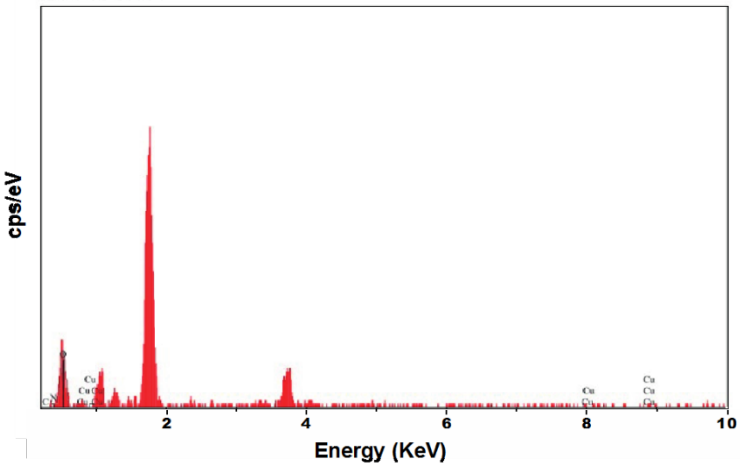

Figure 4. EDAX spectrum of polyCuL2/FTO.

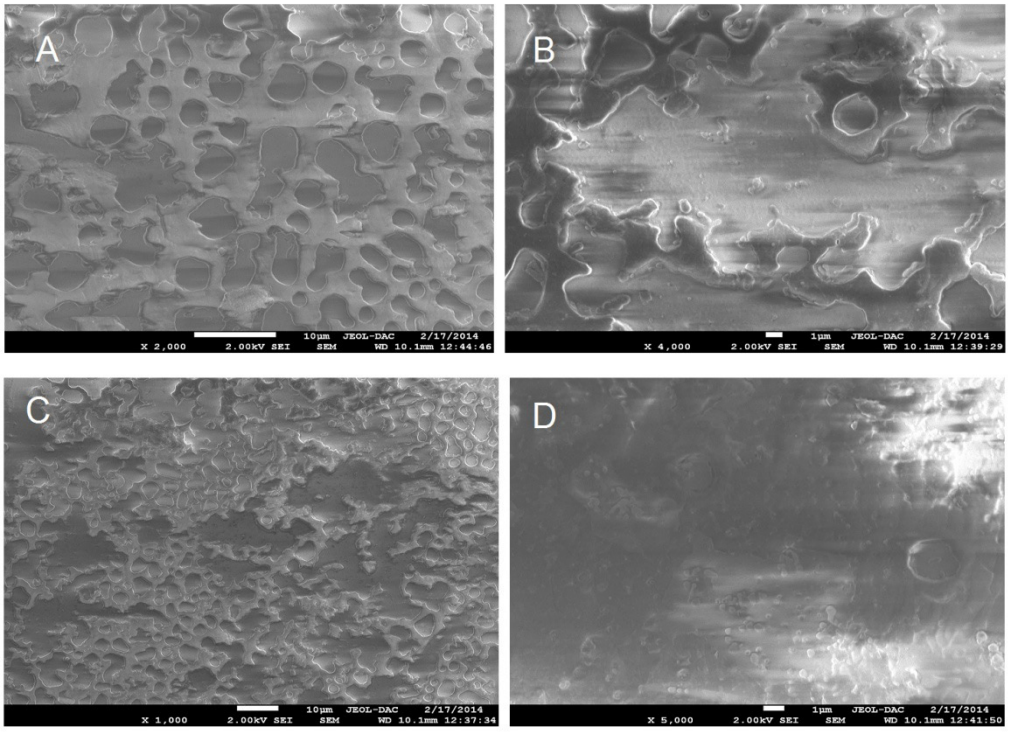

Figure 5. Scanning electron micrographs of the FTO modified electrode surface with polyCuL_2/FTO, (a) X 2.000, 2.0 Kv 10 μm, (b) X 4.000, 2.0 Kv 1 μm (c) X 2.000, 2.00 Kv 10 μm, (d) X 5.000, 2.0 Kv 1 μm.

Catalytic effect of polyCuL$_2$

The electrochemical determination of the efficient catalytic activity for the reduction of oxygen by a CG electrode modified with a polyCuL$_2$ film was conducted in a mixture containing 9.2 mg.L^{-1} of oxygen (O_2) and 0.5 mol.L^{-1} KCl solution (Fig. 6). Under a controlled nitrogen atmosphere, the signal was almost zero (Curve A). However, in an air medium, the signal became significant (Curve B). This indicates that the electrocatalytic efficiency was drastically affected by the modification of the electrode surface, resulting in polyCuL$_2$/GC films [35–37]. The results showed a significant enhancement of the redox system, observed at -0.8 V vs. SCE, which has been attributed to oxygen reduction by the Cu(II)/Cu(I) couple[38].

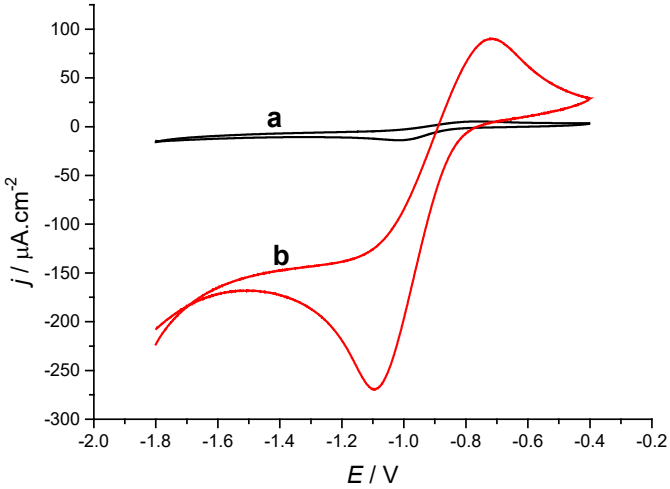

Figure 6. Cyclic voltammograms recorded in 0.1 M TBAP/CH_3CN solution at 100 mV/s with polyCuL$_2$/GC Modified electrode: (a) under saturated nitrogen atmosphere, (b) under saturated air atmosphere.

It is postulated that the catalytic efficiency for a given catalyst can be assessed from the ratios of the cathodic peak (ipc) currents under oxygen and nitrogen atmospheres, denoted as ipc(O_2)/ipc(N_2). As shown in Table 2, higher values for the ipc(O_2)/ipc(N_2) ratios were observed at various scan rates. This indicates a reproducible and efficient electrocatalytic effect, especially at lower scan rates, suggesting that more time allows for the chemical reaction necessary for oxygen reduction [39].

Table 1. Catalytic efficiency data for electrode modified polyCuL$_2$/GC.

Rates (mV/s)	100	75	50	25
$i_{pc}(O_2)/\ i_{pc}(N_2)$	19.28	18.57	20.12	13.67

DNA Binding Study of CuL$_2$ via Cyclic Voltammetry

The cyclic voltammetry technique was applied to study the interaction between the CuL$_2$ complex and DNA. When an increasing concentration of DNA was added to a solution of the CuL$_2$ complex, the anodic peak current height of the complex decreased, and the anodic peak potential exhibited a negative shift. This result suggests that the CuL$_2$ complex interacts with DNA via an electrostatic mode [40]. Cyclic voltammograms of the CuL$_2$ complex in the absence and presence of DNA are shown in Fig. 7a. To avoid acidic or basic denaturation of DNA, the pH of the solution was fixed at the physiological pH of 7.2 using a 0.1 M phosphate buffer solution (KH_2PO_4/K_2HPO_4).

From this observation, it can be noted that in the absence of DNA, the voltammograms of the CuL$_2$ complex show an anodic peak potential at 1.335 V. In the presence of DNA, this peak appears at 1.288 V, with a negative shift of 47 mV, indicating an interaction between the CuL$_2$ complex and DNA. The voltammograms further show a drop in the anodic peak current densities, which can be attributed to the slow diffusion of the DNA–CuL$_2$ adduct [41].

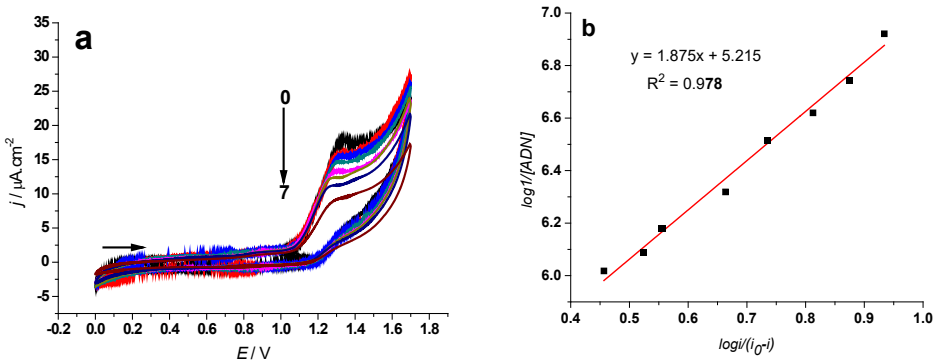

Figure 7. (a) Cyclic voltammograms of 0.1 mM CuL$_2$ in 0.1 M buffer phosphate solution recorded at 0.1 V·s^{-1} potential sweep rate on GC disk electrode in the absence of DNA(0), and in presence of 0.12 (1), 0.24 (2), 0.48 (3), 0.96 (4), 1.44 (5), 1.92 (6) and 2.40 μM DNA (7), **(b)** the plot of $log\ 1/1-(i/i_0)$ versus $log\ 1/[DNA]$ used to calculate the binding constant of ligand CuL$_2$ with DNA.

Binding constant and binding free energy

The decrease in anodic peak current density of the DNA–CuL_2 adduct relative to the free CuL_2 complex is used to calculate the binding constant and binding free energy, using equation 3 [42].

$$\log \frac{1}{[DNA]} = log\, K_b + log \frac{j}{j_0 - j} \quad (3)$$

where j_0 and j are the anodic peak current densities of the free CuL_2 complex and the DNA–CuL_2 adduct, respectively, Kb is the binding constant, and [DNA] is the concentration of the free ligand.

By plotting $log 1/[DNA]$ versus $log 1/1-(j/j_0)$, the binding constant value K_b = 1.33 × 10^5 M^{-1} is obtained from the intercept of the plot, and the binding free energy ΔG =-29.72 kJ.mol^{-1} at ~25 °C is calculated using equation 4.

$$\Delta G = -RT\, ln\, K_b \quad (4)$$

where R is the universal gas constant and T is the temperature in Kelvin.

DNA Binding Study of CuL_2 via molecular docking studies

Molecular docking studies of the CuL_2 complex with DNA were performed to predict the binding site and favored orientation of the ligand within the DNA. The three-dimensional crystal structures of DNA (PDB ID: 1W0T) and the CuL_2 complex (CCDC ID: 1044698) were obtained from the Protein Data Bank (http://www.pdb.org) [43] and The Cambridge Crystallographic Data Centre (https://www.ccdc.cam.ac.uk), respectively.

Before performing the docking calculations, crystallographic water molecules and protein molecules were removed from the DNA crystal structure, hydrogen atoms were added, and partial charges were assigned to the DNA structure file. The PDB file format of the CuL_2 complex structure was obtained from the CIF file and imported into the AutoDock molecular docking software.

Fig. 8 shows the 3D conformation structure of the CuL_2 complex. All docking studies were conducted on a Pentium 3.30 GHz microcomputer with 4.00 GB of RAM and running the Windows 7 operating system.

At the end of the docking runs, various binding energies of the ligand were obtained with their respective conformations. The most stable conformation corresponding to the strongest binding energy was selected as the best pose for docking analysis. The binding energy of the docked structure of the CuL_2 complex with DNA was found to be -29.93 kJ.mol^{-1} at the 19th run. The magnitude of the calculated binding free energy indicates a

high binding affinity between DNA and the CuL_2 complex, our results are in good agreement with the previously published work by Ebtisam Alolayqi and coworkers [44]. A binding constant of 1.75×10^5 M^{-1} at ~25 °C was derived from the binding energy value. The DNA binding propensity of the complex could be attributed to the presence of the imino-phenyl system.

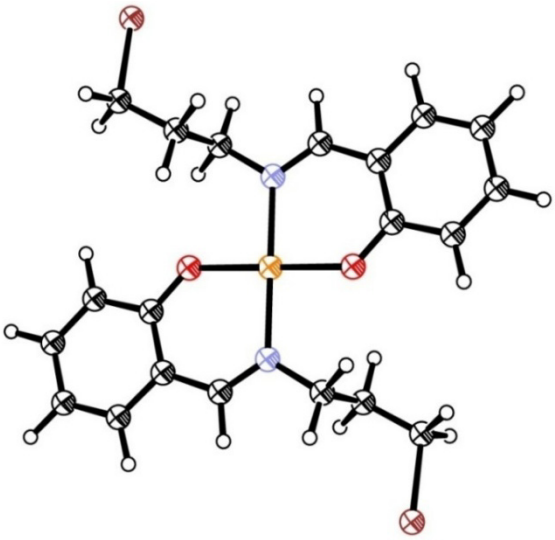

Figure 8. ORTEP of the compound Copper(II) complex of Schiff base N-3-bromopropylsalicylaldimine.

The results indicate that the CuL_2 complex interacts with DNA via its oxygen atom through a hydrogen bond to the hydrogen atom of deoxyadenosine DA11 (Figure 9).

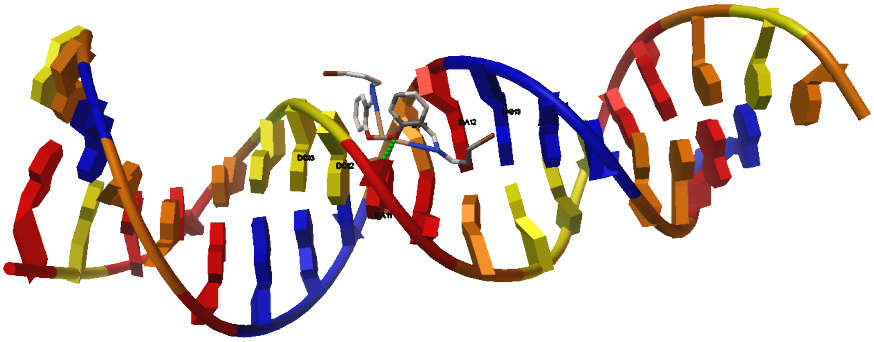

Figure 9. Docking poses of CuL_2 complex with DNA (PDB ID: 1W0T) illustrating the interactions between DNA and the examined complex. It shows the CuL_2 is attached in the minor groove via H-bonding.

CONCLUSIONS

This work describes the electrochemical behavior of the copper(II) complex of the Schiff base, N-3-bromopropylsalicylaldimine, and its electroreduction activity. This complex behaves as a monomer and is easily electropolymerized by an electroreduction process, likely involving radical-radical coupling at the para-positions of the phenoxy groups of the Schiff base moieties or the reduction of C-Br bonds. The efficient electrocatalytic activity of this new material (polyCuL_2) has been demonstrated through its electroreduction in the presence of dioxygen.

Furthermore, the interaction of the copper complex with calf thymus double-stranded (cb-ds) DNA was investigated. DNA interaction studies were conducted using cyclic voltammetry and electronic spectroscopic techniques, and the obtained experimental results were confirmed by molecular docking calculations using the AutoDock 4.2 program. Molecular docking calculations further visualized the interactions and clearly confirmed the groove mode of binding of the Cu(II) complex to cb-ds DNA.

Both experimental results and molecular docking calculations indicated that the CuL_2 complex possesses significant binding affinity with DNA via electrostatic interactions as the dominant mode. Additionally, the magnitude of the binding energy confirms the electrostatic interaction of the studied complex with DNA.

EXPERIMENTAL SECTION

Synthesis

The CuL_2 complex was synthesized following our previously reported procedure [24].

DNA Extraction

DNA was extracted from chicken blood using the Falcon method [45]. The UV absorbance ratio at 260 and 280 nm was 1.97, indicating high purity and minimal protein contamination [45]. The DNA concentration per nucleotide was measured using electronic spectroscopy, applying the known molar extinction coefficient value of 6600 M-1 cm-1 at 260 nm [46].

Cyclic Voltammetry and Software

Cyclic voltammograms were recorded at room temperature (~25 °C) using a mono-compartment cell with a 5 mL capacity. The instrumentation included a VoltaLab 50 Potentiostat/Galvanostat controlled by a microcomputer.

A conventional three-electrode system was used for all experiments in CH_3CN solutions containing 0.1 M TBAP and 0.001 M of the CuL_2 complex to identify the electrochemical profile of the copper complex ligand. For the DNA interaction study, experiments were conducted in phosphate buffer solution at physiological pH 7.2.

The interactions between the CuL_2 complex and DNA were analyzed using the AutoDock 4.2 program [47]. For docking calculations, the AutoDock 4.2 program was used, employing the Lamarckian Genetic Algorithm (LGA) with a genetic algorithm (GA) search. Docking simulations were performed using default parameters, with the number of runs set to 50, 150 individuals, and 2,500,000 energy evaluations. The grid size was set at 70 × 60 × 126 Å, with points separated by 1.000 Å. The grid centers were set at X = 30.562, Y = 37.946, and Z = 18.681. The search was carried out on a grid of 41 and 51 points per dimension with a step size of 0.375 Å, centered on the DNA binding site. The best conformation was selected based on the lowest docking energy.

ACKNOWLEDGMENTS

This work was supported by the directorate-general of scientific research and technological development (DGRSDT) and the laboratory of valorization and technology of Saharan resources (VTRS) (project code: B00L01UN390120150001).

REFERENCES

1. A. Ourari; C. Zoubeidi; W. Derafa; S. Bouacida; H. Merazig; E. Morallon; *Res. Chem. Intermed.*, **2017**, *43*, 3163–3182.
2. A. Ourari; K. Ouari; W. Moumeni; L. Sibous; G. M. Bouet; M. A. Khan; *Transit. Met. Chem.*, **2006**, *31*, 169–175.
3. C. Santos; M. Vilas-Boas; M. F. M. Piedade; C. Freire; M. T. Duarte; B. De Castro; *Polyhedron*, **2000**, *19*, 655–664.
4. A. D. Khalaji; *Curr. Trends X-Ray Crystallogr. Chandrasekaran, Q., Ed.*, **2011**, 161–190.
5. R. K. Parashar; R. C. Sharma; A. Kumar; G. Mohan; *Inorg. Chim. Acta*, **1988**, *151*, 201–208.
6. J. Losada; I. del Peso; L. Beyer; *Transit. Met. Chem.*, **2000**, *25*, 112–117.
7. Z. Li; J.-T. Hou; S. Wang; L. Zhu; X. He; J. Shen; *Coord. Chem. Rev.*, **2022**, *469*, 214695.
8. A. Fazal; S. Al-Fayez; L. H. Abdel-Rahman; Z. S. Seddigi; A. R. Al-Arfaj; B. El Ali; M. A. Dastageer; M. A. Gondal; M. Fettouhi; *Polyhedron*, **2009**, *28*, 4072–4076.
9. L. J. Childs; M. Pascu; A. J. Clarke; N. W. Alcock; M. J. Hannon; *Chem. Eur. J.*, **2004**, *10*, 4291–4300.

10. L. J. Childs; J. Malina; B. E. Rolfsnes; M. Pascu; M. J. Prieto; M. J. Broome; P. M. Rodger; E. Sletten; V. Moreno; A. Rodger; *Chem. Eur. J.*, **2006**, *12*, 4919–4927.
11. A. A. Amer; H. Ilikti; C. Beyens; J. Lyskawa; U. Maschke; *Eur. Polym. J.*, **2019**, *112*, 569–580.
12. A. Ourari; B. Ketfi; S. I. R. Malha; A. Amine; *J. Electroanal. Chem.*, **2017**, *797*, 31–36.
13. G. Mahalakshmi; K. N. Vennila; B. Selvakumar; P. L. Rao; R. Malwade; S. Deval; S. Madhuri; M. Seenivasaperumal; K. P. Elango; *J. Biomol. Struct. Dyn.*, **2020**, *38*, 3443–3451.
14. P. U. Maheswari; M. Palaniandavar; *J. Inorg. Biochem.*, **2004**, *98*, 219–230.
15. C. Metcalfe; J. A. Thomas; *Chem. Soc. Rev.*, **2003**, *32*, 215–224.
16. K. Abdi; H. Hadadzadeh; M. Weil; M. Salimi; *Polyhedron*, **2012**, *31*, 638–648.
17. H. Hadadzadeh; M. Salimi; M. Weil; Z. Jannesari; F. Darabi; K. Abdi; A. D. Khalaji; S. Sardari; R. Ahangari; *J. Mol. Struct.*, **2012**, *1022*, 172–180.
18. S. Dhar; F. X. Gu; R. Langer; O. C. Farokhzad; S. J. Lippard; *Proc. Natl. Acad. Sci.*, **2008**, *105*, 17356–17361.
19. S. Dhar; Z. Liu; J. Thomale; H. Dai; S. J. Lippard; *J. Am. Chem. Soc.*, **2008**, *130*, 11467–11476.
20. I. M. A. Mohamed; A. M. Abu-Dief; **2015**.
21. S. Sathiyaraj; G. Ayyannan; C. Jayabalakrishnan; *J. Serbian Chem. Soc.*, **2014**, *79*, 151–165.
22. T. J. Kistenmacher; T. Sorrell; L. G. Marzilli; *Inorg. Chem.*, **1975**, *14*, 2479–2485.
23. J. A. Carrabine; M. Sundaralingam; *J. Am. Chem. Soc.*, **1970**, *92*, 369–371.
24. A. Ourari; C. Zoubeidi; S. Bouacida; W. Derafa; H. Merazig; *Acta Crystallogr. Sect. E Crystallogr. Commun.*, **2015**, *71*, m33–m34.
25. S. Rayati; S. Zakavi; M. Koliaei; A. Wojtczak; A. Kozakiewicz; *Inorg. Chem. Commun.*, **2010**, *13*, 203-207.
26. F. Bedioui; E. Labbe; S. Gutierrez-Granados; J. Devynck; *J. Electroanal. Chem.*, **1991**, *301*, 267-274.
27. A. Jozwiuk; Z. Wang; D. R. Powell; R. P. Houser; *Inorg. Chim. Acta,* 394 (2013) 415–422
28. M. Roelsgaard; P. Nørby; E. Eikeland; M. Søndergaard; B. B. Iversen; *Dalt. Trans.*, **2016**, *45*, 18994–19001.
29. M. Vilas-Boas; C. Freire; B. De Castro; A. R. Hillman; *J. Phys. Chem. B*, **1998**, *102*, 8533–8540.
30. H. Kianfar; L. Keramat; M. Dostani; M. Shamsipur; M. Roushani; F. Nikpour; *Spectrochim. Acta Part A Mol. Biomol. Spectrosc.*, **2010**, *77*, 424–429.
31. C. S. Martin; T. R. L. Dadamos; M. F. S. Teixeira; *Sensors Actuators B Chem.*, **2012**, *175*, 111–117.
32. T. R. L. Dadamos; M. F. S. Teixeira; *Electrochim. Acta*., **2009**, *54*, 4552–4558.
33. I. A. Chepurnaya; M. P. Karushev; E. V Alekseeva; D. A. Lukyanov; O. V Levin; *Pure Appl. Chem.*, **2020**, *92*, 1239–1258.
34. P. Audebert; P. Hapiot; P. Capdevielle; M. Maumy; *J. Electroanal. Chem.*, **1992**, *338*, 269–278.

35. J. H. Cameron; S. C. Turner; *J. Chem. Soc. Dalt. Trans.*, **1992**, 3285–3289.
36. A. Pui; I. Berdan; I. Morgenstern-Badarau; A. Gref; M. Perrée-Fauvet; *Inorg. Chim. Acta*, **2001**, *320*, 167–171.
37. J.-C. Moutet; A. Ourari; *Electrochim. Acta*, **1997**, *42*, 2525–2531.
38. M. Martins; M. V. Boas; B. de Castro; A. R. Hillman; C. Freire; *Electrochim. Acta*, **2005**, *51*, 304–314.
39. M. A. Thorseth; C. E. Tornow; C. M. Edmund; A. A. Gewirth; *Coord. Chem. Rev.*, **2013**, *257*, 130–139.
40. N. Li; Y. Ma; C. Yang; L. Guo; X. Yang; *Biophys. Chem.*, **2005**, *116*, 199–205.
41. A. Shah; M. Zaheer; R. Qureshi; Z. Akhter; M. F. Nazar; *Spectrochim. Acta Part A Mol. Biomol. Spectrosc.*, **2010**, *75*, 1082–1087.
42. G.-C. Zhao; J.-J. Zhu; J.-J. Zhang; H.-Y. Chen; *Anal. Chim. Acta*, **1999**, *394*, 337–344.
43. P. W. Rose; A. Prlić; A. Altunkaya; C. Bi; A. R. Bradley; C. H. Christie; L. Di Costanzo; J. M. Duarte; S. Dutta; Z. Feng; et al.; *Nucleic Acids Res.*, **2017**, *45*, D271–D281.
44. E. Alolayqi; M. Afzal; A. Alarifi; A. Beagan; M. Muddassir; *Crystlals*., **2022**, 12(1), 15.
45. E. Lanez; L. Bechki; T. Lanez; *Chem. Chem. Technol.*, **2019**, *13*, 11–17.
46. T. Lanez; H. Benaicha; E. Lanez; M. Saidi; *J. Sulfur Chem.*, **2018**, *39*, 76–88.
47. R. Vijayalakshmi; M. Kanthimathi; V. Subramanian; B. U. Nair; *Biochem. Biophys. Res. Commun.*, **2000**, *271*, 731–734.
48. C. Steffen; K. Thomas; U. Huniar; A. Hellweg; O. Rubner; A. Schroer; *J. Comput. Chem.*, **2010**, *31*, 2967–2970.